In-Channel Electrochemical Detection in the Middle of Microchannel under High Electric Field

ARTICLE *in* ANALYTICAL CHEMISTRY · DECEMBER 2011

Impact Factor: 5.64 · DOI: 10.1021/ac2016322 · Source: PubMed

6 AUTHORS, INCLUDING:

Segyeong Joo
Asan Medical Center
40 PUBLICATIONS **428** CITATIONS
SEE PROFILE

Je Hyun Bae
City University of New York - Queens College
21 PUBLICATIONS **104** CITATIONS
SEE PROFILE

Yang-Rae Kim
Seoul National University
45 PUBLICATIONS **803** CITATIONS
SEE PROFILE

analytical chemistry

Article

pubs.acs.org/ac

In-Channel Electrochemical Detection in the Middle of Microchannel under High Electric Field

Chung Mu Kang,[†] Segyeong Joo,[‡] Je Hyun Bae,[†] Yang-Rae Kim,[†] Yongseong Kim,[§] and Taek Dong Chung*,[†]

[†]Department of Chemistry, Seoul National University, Seoul 151-747, Korea

[‡]Department of Medical Engineering, Asan Medical Center, University of Ulsan College of Medicine, Seoul 138-736, Korea

[§]Department of Science Education, Kyungnam University, Masan 631-701, Korea

Supporting Information

ABSTRACT: We propose a new method for performing in-channel electrochemical detection under a high electric field using a polyelectrolytic gel salt bridge (PGSB) integrated in the middle of the electrophoretic separation channel. The finely tuned placement of a gold working electrode and the PGSB on an equipotential surface in the microchannel provided highly sensitive electrochemical detection without any deterioration in the separation efficiency or interference of the applied electric field. To assess the working principle, the open circuit potentials between gold working electrodes and the reference electrode at varying distances were measured in the microchannel under electrophoretic fields using an electrically isolated potentiostat. In addition, "in-channel" cyclic voltammetry confirmed the feasibility of electrochemical detection under various strengths of electric fields (~400 V/cm). Effective separation on a microchip equipped with a PGSB under high electric fields was demonstrated for the electrochemical detection of biological compounds such as dopamine and catechol. The proposed "in-channel" electrochemical detection under a high electric field enables wider electrochemical detection applications in microchip electrophoresis.

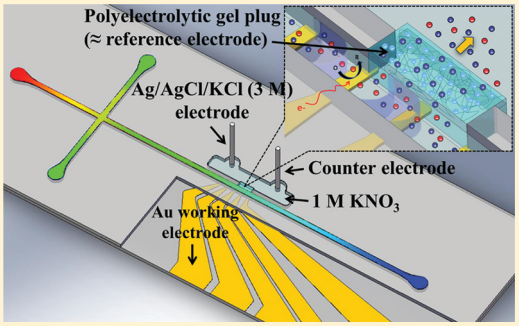

Over the past decade, microchip electrophoresis (MCE) has emerged as an attractive method for chemical and biological analysis using miniaturized systems.[1−3] With the aim of enabling nonexperts to carry out ubiquitous analysis, recent applications of microfluidic chip-based analytical tools tend toward the integration of multiple unit processes such as sample pretreatment, separation, and detection into a single chip.[4,5] Of the necessary elements for portable systems, the detection technique is key for a high-performance separation-based system with low detection limits, fast analysis, high throughput, low cost, disposability, and portability.[6,7] A detector that can be truly miniaturized would offer immeasurable benefits for chip-based analytical tools.

Many attempts to incorporate detection methods such as Fourier transformation of infrared light absorption spectra (FT-IR), Raman scattering, nuclear magnetic resonance (NMR), refractive index (RI), thermal lens microscopy (TLM), microplasma-optical emission spectroscopy (OED), surface plasmon resonance (SPR), electrochemical analysis (EC), chemiluminescence (CL), mass spectrometry (MS), UV−vis absorbance (UV−vis), and laser induced fluorescence (LIF) into electrophoresis devices have been reported.[8−10] In particular, much attention has been focused on MS, LIF, UV−vis, and EC because of their compatibility with the capillary electrophoresis (CE) technique without a significant loss in detection quality. Although the majority of commercial CE instruments employ UV−vis absorbance, this method is unsuitable for trace chemical analysis in the nanomolar or below-nanomolar concentration range due to its inherently poor detection limit.[11] MS detection reportedly offers high throughput in conjunction with the MCE;[12] however, it is expensive and usually not portable. LIF is a common detection method that allows extremely sensitive detection in combination with a MCE.[13,14] However, it is necessary to select natural fluorescent compounds which must be derivatized with a fluorophore to perform a LIF method. The EC detection method comprises very simple instrumentation and integration of microscale electrodes onto a microchip,[15] while maintaining excellent sensitivity and selectivity.[16] As a result, it has been intensively employed as the ideal detection method in microfluidic on-chip separation systems.[17] The largest challenge with respect to EC detection is the influence of the high CE voltage and current on the detector, which causes severe noise and can make electrochemical detection impossible.[18−20] Furthermore, an electrical surge may critically damage the EC detector.[21]

Received: June 26, 2011
Accepted: December 13, 2011
Published: December 13, 2011

Amperometric detection methods are classified into end-channel and in-channel types, depending on the position of the working electrode in a microchannel.[22] End-channel detection is a facile method to measure redox current from analytes that reduces the influence of the CE voltage and current. Woolley et al.[23] proposed end-channel detection on a microchip that was placed in a gradually widening separation channel just before the working electrodes in order to minimize the interference of the CE field. However, measuring the electrochemical current near the outlet of the channel induces a shift in the half-wave potential of the redox couple, which results in poor reproducibility due to the sensitivity toward the relative position of the working electrode and the channel outlet under the CE field. To solve this problem, Wang et al.[24] developed an end-channel detection method called the "wall-jet," which maintains specific distance between the separation channel and the working electrode. However, the structure of the separation channel connected to the perpendicular detector strip limits the miniaturization and versatility of the microchip. Although end-channel detection provides a method to measure EC current under a CE field, it still has a few practical problems including sample plug dispersion, which causes peak broadening and affects separation efficiency. Ertl et al.[25] improved end-channel detection by focusing a sample plug with a sheath-flow supported microchip. However, the creation of sheath-flow channels increases the complexity of the channel design. Several theoretical and experimental strategies to measure the redox current from analytes within a separation channel have been reported.[26−28] Martin et al.[29] reported a design with the working electrode aligned at the very end of, but still inside, the separation channel. However, this in-channel arrangement demands precise alignment of the working electrode in the separation channel to minimize the shift of the half-wave potential and electrochemical noise. Chen et al.[30] proposed in-channel detection to eliminate the potential shift using a dual-channel configuration; however, the working and reference electrodes must be placed as close as possible to the counter electrode, which is located at the channel outlet, to minimize *iR* drop. In addition, the dual-channel in this detection scheme requires complex channel design that hinders the simplification of chip patterns and makes integration of other components onto the same chip difficult.

The decoupling approach is another strategy to isolate the amperometric signals from the CE field and eliminate the diffusive band-broadening that is observed in the end-channel strategies. Rossier and co-workers[31] reported the integration of a decoupler composed of a microhole array located perpendicular to the separation channel. Chen et al.[32] utilized a palladium metal electrode as a decoupler to effectively dissipate the hydrogen bubbles. Although these decoupling methods for in-channel detection offer another effective way to isolate the EC detector from the separation field and suppress the band broadening that is characteristic of end-channel methods, band dispersion still exists due to the rapid decrease of the electric field strength between the decoupler and working electrode.[33] Another approach that employs bipolar electrochemistry[34,35] is an in-channel detection method without a decoupler. However, the amperometric detection method-based bipolar electrochemistry,[36,37] which controls the potential of the working electrode by adjusting the bipolar electrode size, electrode gap, or the electric field strength, is not appropriate for the detection of redox-active analytes with different redox potentials.

In this paper, we propose a new strategy that allows in-channel detection by the placement of a novel polyelectrolytic gel salt bridge (PGSB) between the reference and working electrodes on the equipotential surface of the separation channel (Scheme 1). This in-channel method is particularly

Scheme 1. Schematic of the PGSB-Integrated MCE[a]

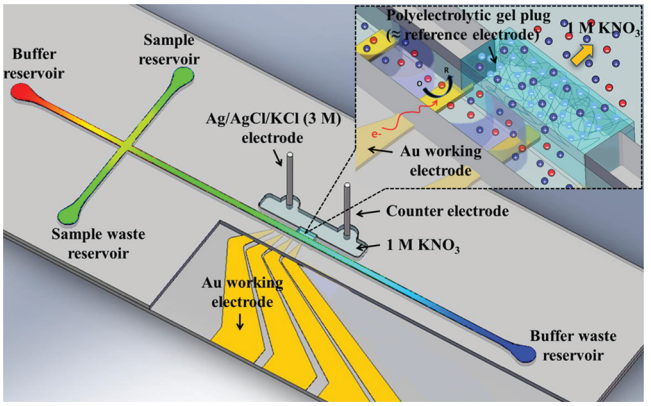

[a]The Au working electrode and polyelectrolytic gel plug, which is electrically linked to the reference electrode system through the internal filling solution, are on an equipotential surface in the channel under an electrophoretic field. The color distribution from red to blue in the channel represents the electrophoretic field gradient that was calculated using computational fluid dynamics (CFD) software, i.e., CFD-ACE+ (CFD Research Corp.). Inset: Schematic representation of the configuration of a PGSB/Au electrode for in-channel amperometric detection on the microchip.

suitable for MCE for the following reasons: (i) In-channel detection is easily accomplished without a decoupler. (ii) The generation of PGSB by UV exposure is very simple and, thus, the PGSB can be placed anywhere in the separation channel. (iii) The electrically isolated detector obviates damage to the electronics, thereby minimizing potential fluctuation at the working electrode. (iv) The placement of the working electrode in the separation channel allows for high separation efficiency by eliminating the band-broadening that is observed when end-channel detection is used. (v) The placement of the working and reference electrodes on an equipotential surface substantially reduces the shift of the half-wave potential and the background noise; therefore, a constant potential can be applied to the working electrode even under varying and possibly fluctuating CE fields.

EXPERIMENTAL SECTION

Chemicals and Reagents. A 2.5 M aqueous solution of 2-acrylamido-2-methyl-1-propanesulfonic acid (AMPSA) was used in combination with 1% 2-hydroxy-4′-(2-hydroxyethoxy)-2-methylpropiophenone as a photoinitiator and 0.5% *N*,*N*′-methylenebisacrylamide as a cross-linker to fabricate the polyelectrolytic gels. A solution of 3-(trimethoxysilyl)propyl methacrylate (TMSMA) in anhydrous methanol was used as the coating material for adhesion of the polyelectrolytic gels onto the surface of the channels. Stock solutions of varying concentrations of potassium ferricyanide in 100 mM potassium nitrate were prepared as a supporting electrolyte for potentiometric measurements. The electrophoresis buffer solution of the potassium ferricyanide was 25 mM sodium borate. A solution containing neurotransmitters such as

dx.doi.org/10.1021/ac2016322 | *Anal. Chem.* 2012, 84, 901−907

dopamine and catechol was prepared in a 25 mM 2-(*N*-morpholino)ethanesulfonic acid (MES) buffer solution with a pH of 6.5. All the reagents were purchased from Sigma-Aldrich (USA).

Fabrication of a PGSB Integrated Microchip. The MCE device depicted in Figure 1 was fabricated using traditional photolithographic techniques, UV epoxy bonding, and novel photopolymerization of the polyelectrolytic gel plug by UV exposure. The patterning of the channel and the Au electrode were prepared similarly to our previous work.[38,39] In brief, for the formation of the microchannel pattern, a glass cover slide (Cat. No. 1000412, Paul Marienfeld GmbH & Co. KG, Germany) was initially cleaned using a piranha solution (H_2SO_4/H_2O_2 = 3:1). (*Caution: The piranha solution should be handled with extreme care because it is a powerful oxidizing agent that reacts violently with organic compounds.*) Photoresist (AZ4620, Clariant, Switzerland) was spin-coated at 7000 rpm for 30 s onto the glass slide. It was then sequentially treated with photolithography procedures including soft baking, UV exposure, development, hard baking, and wet etching.

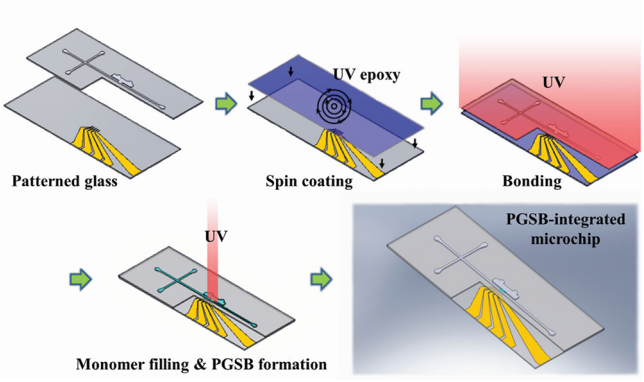

Figure 1. Fabrication of the PGSB on a glass microchip. UV bonding was rapid and allowed the use of a glass chip, which guarantees stability of the electrode. The PGSB was formed by UV exposure immediately after bonding.

A similar photolithographic protocol was applied to prepare the bottom glass slide. After cleaning the glass slide with the piranha solution and coating it with hexamethyldisilazane (HMDS; Clariant, Switzerland), AZ5214 (Clariant, Switzerland) was spin-coated at 4000 rpm for 30 s. Prebaking for 1 min at 100 °C was followed by a first exposure for 5 s at 17 mJ/cm^2, reversal baking for 5 min at 100 °C, flood exposure for 20 s at 17 mJ/cm^2, and development using AZ300MIF (Clariant, Switzerland). Metal films were sputtered on the patterned glass using a DC/RF magnetron sputter (Atek, Korea). An adhesion layer of titanium (Ti) was sputtered to a thickness of approximately 350 Å. A gold (Au) film 5000 Å thick and 10 or 20 μm wide was deposited at 5 Å/s onto the Ti layer. The Au-patterned glass was then immersed into acetone (J.T. Baker, USA) to remove the remainder of the patterned Au/Ti layer. UV exposure was used for the subsequent bonding procedure and PGSB integration. After cleaning with piranha solution and air blowing, the Au electrode pattern was spin-coated with a UV curing resin (LOT No. A10K01, ThreeBond Co., Ltd., Japan) at 1500 rpm for 30 s. The substrate was exposed to 365 nm UV light for 12 s at 17 mJ/cm^2. The channels were then flushed with acetone for 30 s. The bottom glass slide was electrochemically cleaned by cycling the potential between +1.0 and +0.2 V in 0.5 M H_2SO_4 using an Ag/AgCl and a Pt wire as the reference and counter electrodes, respectively. An optical image of the microchip is shown in the Supporting Information Section A.

The final chip was prepared by bonding the cover and bottom glass slides. After cleaning with H_2SO_4, the surface areas of the Au electrodes that were exposed to the microchannel were experimentally checked to confirm that the Au thin film acted as electrodes and was stable. The Au surface areas were measured by cyclic voltammetry in a 5 mM $K_3Fe(CN)_6$ solution and found to be consistent with the areas measured using a video microscope system (ICS-305B, Sometech, Korea) (Supporting Information Section B). The PGSB in the channel was fabricated using UV exposure. In brief, the channels in the microfluidic chip were filled with 0.1 M TMSMA solution and stored at room temperature for 20 min. Before being washed with anhydrous methanol and filled with a 2.5 M AMPSA monomer solution, the microfluidic chip was exposed to UV light through a photomask for 35 s at 17 mJ/cm^2. Finally, the Au surface was electrochemically polished by cycling the potential between +1.0 and +0.2 V versus Ag/AgCl in 0.5 M H_2SO_4 until reproducible cyclic voltammograms were obtained. To confirm the effect of cleaning the Au electrode surface with H_2SO_4, the electrochemical behavior was checked using a TMSMA-modified gold substrate as the control. The cyclic voltammograms shown in Supporting Information Section C indicate that the Au surface was clarified by cleaning with H_2SO_4.

Instruments. Electrochemical examination of the Au electrodes on the chip was carried out using a conventional potentiostat (Model CHI660A, CH Instruments Inc.) with an Ag/AgCl electrode and a Pt wire as the reference and counter electrodes, respectively. A DBHV-100 high voltage supplier (Digital Bio Technology, Korea) driven by a six-channel voltage control program, which was written using LabVIEW software version 8.2 (National Instruments, Austin, TX), was used for electrophoresis. The potentiostat was isolated from the external electric outlet by a custom-made DC power supplier that converted from DC 9 V batteries to DC +5, +15, and −15 V to match the output voltages of the internal power module of the potentiostat. Amperometric detection was performed in a Faraday cage equipped with a picoamp booster (Model CHI200, CH Instruments Inc.).

Electrophoresis. To optimize the surface condition of the microchannels, the glass chip channel was treated according to the following procedure. First, the channel was rinsed with deionized water, 0.1 M HCl, 0.1 M NaOH, and 25 mM $Na_2B_4O_7$ (or 25 mM MES) for 10 min each. The effect of the position of the Au working electrode relative to the PGSB was evaluated by through electrophoretic separation of the ferricyanide species. A 200 μM potassium ferricyanide solution was placed in the sample reservoir and loaded in the pinched injection mode by applying +150 V to the sample waste reservoir for 20 s; the sample reservoir was grounded while both the buffer and waste reservoirs were floating. For sample injection and separation, voltages of +250 and +100 V were applied to the buffer−waste reservoir and the sample reservoir/sample−waste reservoir, respectively, and the buffer reservoir was grounded. The detection potential of +0.15 V (vs an Ag/AgCl/KCl (3M) reference electrode located in the chamber beyond the PGSB, as shown in Scheme 1) was applied to the Au working electrode during the separation.

dx.doi.org/10.1021/ac2016322 | *Anal. Chem.* 2012, 84, 901−907

To ensure successful electrophoresis and amperometric detection under the high electric field, two biological compounds, i.e., 100 μM dopamine and 150 μM catechol, were mixed in a 25 mM MES buffer. Similar to the method that was used to load and separate ferricyanide, pinched injection was employed to load the sample plug by applying +150 V between the sample and the sample waste reservoir for 20 s. The separation was carried out under a variety of electric fields (50−500 V/cm).

RESULTS AND DISCUSSION

Open Circuit Potential under an External Electric Field. The open circuit potential (OCP) between the Au working electrodes and the PGSB was measured under various electric fields. Figure 2 shows the OCP data obtained with

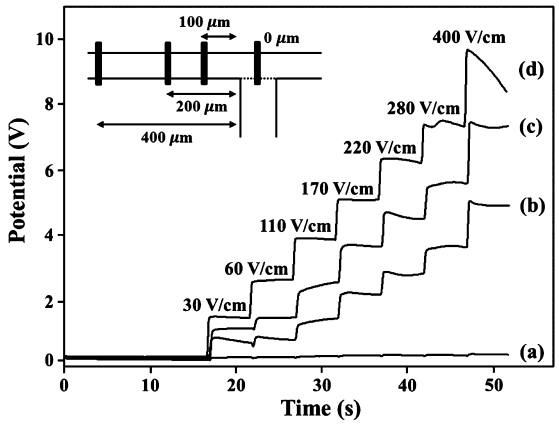

Figure 2. Open circuit potential difference as a function of the relative position of the Au working electrode and the PGSB under various electrophoretic fields. The Au working electrodes (10 μm wide) were (a) 0 μm, (b) 100 μm, (c) 200 μm, (d) and 400 μm away from the PGSB, as shown in the inset. The microchannel was filled with 100 mM KNO_3 solution.

spaces of −0, 100, 200, and 400 μm between the Au working electrodes and the PGSB. The electric field gradient (ΔV_s) applied along the microchannel for electrophoretic separation varied from 30 to 400 V/cm. The OCP data was obviously dependent on the ΔV_s as well as the distance between the Au working electrode and the PGSB. The OCP increased with increasing ΔV_s and distance. This result indicates that there are critical problems that need to be solved in order to perform electrochemical detection using electrodes in the middle of a microchannel with a high electric field for electrophoresis.

There are two primary problems: (1) the bipolar disparity of the electrochemical potential on the electrode and (2) inaccurate amperometric detection. The first issue is closely linked to the bipolar effect that is observed when an electrode is exposed to a steep electric field gradient. This bipolar electrode behavior[40−42] may distort electrochemical signals from the electrode and harm the working electrode surface. A steep gradient of the external electric field in the solution phase may lead to considerable disparity in the electrochemical potential between the ends of an electrode (ΔV_{edge}). However, the Fermi level throughout the electrode is not expected to be significantly affected by the field gradient. This disparate electrochemical potential on the electrode surface is a function of the width and position of the electrode on the microfluidic chip. A larger ΔV_{edge} is observed for wider electrodes that are further from the PGSB in the narrow microchannel. The maximum voltage, applied to the microchannel for electrophoretic separation, is restricted by the condition that no wireless electrochemical reaction should take place due to the external electric field gradient. To satisfy this condition, ΔV_{edge} should be lower than the electrochemical potential window for a given solution and electrode material.

The potential window is determined via a cyclic voltammogram obtained in the absence of the electric field gradient in the solution. For example, an electric field with a strength of 400 V/cm causes a maximum difference of 0.4 and 0.8 V between the edges of 10 and 20 μm wide Au electrodes, respectively. Because the potential window of the Au electrode in the 0.1 M KNO_3 and MES buffer employed in this study is wider than 1 V, the electrochemical reaction on the Au electrode due to the external electric field required for electrophoretic separation would be negligible. Moreover, as Figure S4 in Supporting Information Section D illustrates, the electric potential gradient is expected to be minimal in front of the PGSB, which is connected to a reference electrode system with a very low resistance. The reduction of the electric potential gradient near the PGSB leads to a minimal bipolar effect, i.e., suppression of ΔV_{edge}, if the electrode is positioned just in front of the PGSB. This was confirmed by the significant reduction in OCP fluctuation, as shown in Figure 2a.

The other problem is the accuracy of the electrochemical potential that is applied to the Au electrode for amperometric detection. This is also a function of ΔV_{edge} and the potential drop between the electrode and the PGSB. It is evident that a higher resistance between the working and the reference electrodes under a steeper external electric field would produce a larger potential drop along the solution in the microchannel.[43] Therefore, it is necessary to tune the position of the working electrode with respect to the PGSB for successful amperometric detection during electrophoresis on a microchip. Practically, the potential shifts between the working and reference electrodes that are caused by ΔV_s in the microchannel can be calibrated using a hydrodynamic voltammogram.[44] However, the position within the microchannel that is significantly away from the PGSB is still problematic. First, the electrochemical potential is unavoidably affected by the ΔV_s, which is normally on a much larger scale than the potential difference applied between the working and reference electrodes for amperometric detection. Even a tiny fluctuation in ΔV_s can result in a severe shift in the electrochemical potential for amperometric detection. Moreover, this system is also affected by the bipolar effect, i.e., ΔV_{edge}. Due to the significantly reduced electric potential gradient near the PGSB, the electrode just in front of the PGSB is predicted to be on an almost equipotential surface with the PGSB. Therefore, the solution potential at the working electrode located near the PGSB is not significantly different from that of the reference electrode (Supporting Information Section D). This is supported by the fact that the potential fluctuation in OCP (ΔV_F) was less than 5 mV even under a high external electric field (ΔV_s) of 400 V/cm (Supporting Information Section E). These results are in good accordance with the Klett report,[45] which showed the OCP data that was acquired on an equipotential surface. These results indicate that the working electrode located just in front of the PGSB has the same potential as the reference electrode when no potential bias is applied for amperometric detection. The potential fluctuation is minimized, and the noise level is effectively suppressed. Therefore, if the electrode is located just in front of

dx.doi.org/10.1021/ac2016322 | Anal. Chem. 2012, 84, 901−907

the PGSB, there is no need for the enormous increase of detection potential to compensate for the effect of ΔV_s.[29,43,46] Consequently, placing the working electrode close to the PGSB enables accurate control of the electrochemical potential in the middle of the electrophoretic channel, which allows for continuous amperometric detection during electrophoresis.

Cyclic Voltammetry under Various Electric Fields. The electric potential gradient in the middle of the microchannel is proportional to the resistance of the region of interest on the microchip.[47] The local resistance in the region in front of the PGSB is significantly less than in other parts of the microchannel because the PGSB is an electric conductor that enables free migration of ions and is linked to the reference electrode. The potential drop near the PGSB is expected to deviate from the linearity of the electric potential in the remainder of the microchannel (Supporting InformationSection D). This prediction was confirmed by the OCP data shown in Figure 2, which were acquired from the electrode placed in front of the PGSB and are almost free from the effects of the external potential gradient. Noise generated during the potentiometric measurement increased proportionally with the external electric field (ΔV_s). Nevertheless, the noise level was less than 5 pA in the Faraday cage. The cyclic voltammograms shown in Figure 3 indicate that the electrochemical redox

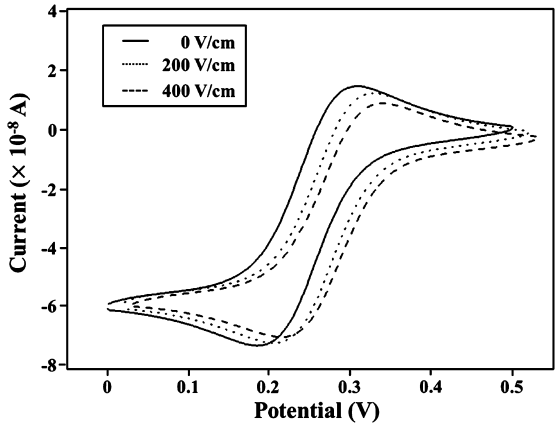

Figure 3. Cyclic voltammograms from the Au electrode located in front of the PGSB under CE fields: solid line (0 V/cm), dotted line (200 V/cm), and dashed line (400 V/cm). Cyclic voltammetry was performed in a 1 mM $K_3Fe(CN)_6$ solution with 100 mM KNO_3 (supporting electrolyte). Conditions: width of the Au working electrode, 10 μm; reference electrode, Ag/AgCl/KCl (3 M); counter electrode, Pt wire; scan rate, 100 mV/s.

behavior of the ferricyanide ions at the electrode remain unchanged except for a slight reduction in current and a potential shift of less than several tens of mV under an electric field up to 400 V/cm. This supports that the potential shift and noise resulting from the given range of ΔV_s[48−50] are acceptable for in-channel electrochemical detection during electrophoretic separation on a microchip.

As the distance between the working electrode and the PGSB increases, the EC measurements increasingly suffer from severe noise and inaccurate electrochemical potential of the electrode, which may eventually damage the working electrode (Supporting Information Section F). Therefore, the placement of the working electrode close to the PGSB overcomes the restrictions on amperometric detector position in terms of electrophoresis and allows versatile designs of the microfluidic chip.

Separation on a PGSB Integrated Microchip. Electrophoresis on a microchip equipped with the PGSB was performed to elucidate the separation and detection performances via the separation efficiency and amperometric response. Figure 4 shows the electropherograms from the Au microband

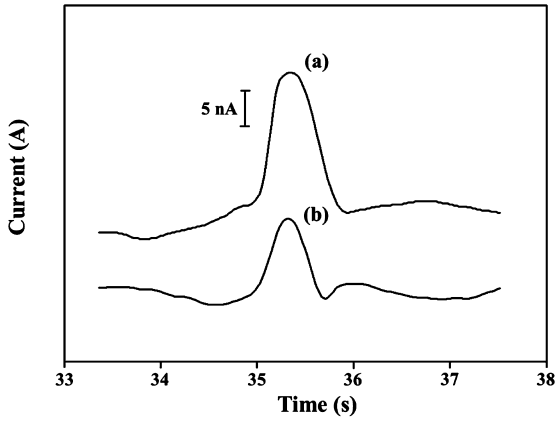

Figure 4. Electropherograms of 200 μM $K_3Fe(CN)_6$ detected (a) 0 μm and (b) 50 μm from the PGSB. Conditions: CE field strength, −150 V/cm; Au working electrode width, 20 μm; total length, 1.6 cm; effective length, 1.2 cm; running buffer, 25 mM sodium borate; detection potential, +0.15 V vs Ag/AgCl/KCl (3 M) reference electrode.

electrodes located (a) 0 and (b) 50 μm from the PGSB. These electropherograms were obtained from the separation of 200 μM potassium ferricyanide at 150 V/cm on a PGSB-integrated microchip. The numbers of theoretical plates (i.e., separation efficiency) were 10 700/m (a) and 11 500/m (b), and the peak currents were 17 nA (a) and 8.0 nA (b). The roles of the polyelectrolytic gel were as an in-channel salt bridge electrically linked to the reference electrode and as a stopper to prevent leakage of the buffer solution.

Although the polyelectrolytic gel is obviously a different material than glass, there are no significant differences between the two regions in terms of separation efficiency. For example, the number of theoretical plates measured using the electrode in front of the PGSB were similar to that from the other electrode, which was located 50 μm away from the PGSB. On the other hand, the peak current was twice as high for the electrode located in front of the PGSB than that of the electrode 50 μm from the PGSB. Figure 4 shows that the peak shape of the electropherogram from the electrode just in front of the PGSB was very similar to that from the electrode in the middle of the glass microchannel. The limit of detection (S/N = 2) was determined to be 1.5 μM for ferricyanide under −150 V/cm (Supporting Information Section G).

Figure 5 demonstrates the functionality of the proposed microchip system equipped with PGSB for neurotransmitter separation by electrophoresis. The electropherograms of the neurotransmitter mixtures consisting of dopamine (100 μM) and catechol (150 μM) show separation under electric fields ranging from 50 to 500 V/cm. The results shown in Figure 5 indicate that the electric field strength was the dominant parameter for determining the separation efficiency. The highest separation efficiency was observed under an electric field of 200 V/cm (catechol, 10 500/m, and dopamine, 8500/m). As the electric field increases from 50 V/cm to 500 V/cm, the migration time decreases for all compounds. The

dx.doi.org/10.1021/ac2016322 | Anal. Chem. 2012, 84, 901−907

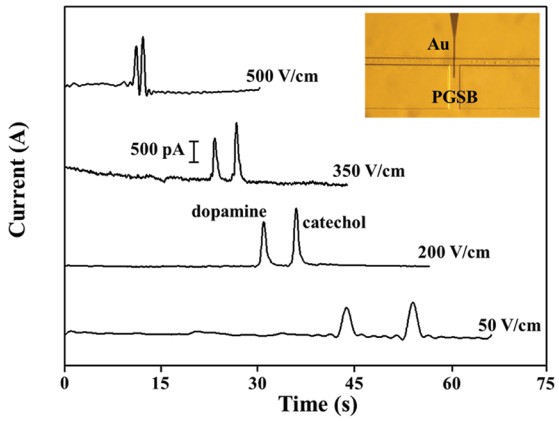

Figure 5. Electropherograms of dopamine (100 μM) and catechol (150 μM) under high electric fields obtained using the PGSB-integrated microchip. Conditions: width of the Au working electrode, 20 μm; total length, 5.4 cm; effective length, 5 cm; running buffer, 25 mM MES; detection potential, +0.05 V vs Ag/AgCl/KCl (3 M) reference electrode.

reproducibility of electrophoresis on the PGSB integrated microchip was evaluated by performing 7 repetitive separations. Mean migration times of 32 s (±0.8) and 36 s (±1.2) and peak currents of 750 pA (±40) and 920 pA (±35) were observed for dopamine and catechol, respectively. These electrophoresis results confirm reproducibly a separation under a high electric field employing a PGSB-based detection system.

CONCLUSIONS

A novel in-channel electrochemical detection method for MCE based on a polyelectrolytic gel salt bridge was proposed and validated. This configuration enables in-channel electrochemical detection with very limited interference of the applied electrophoretic field by the introduction of a PGSB. Besides enabling electrochemical detection under various high electric fields, the simple fabrication process of the concise glass microchip ensures promising applications for portable and reliable MCE devices. Consequently, this method represents a technical breakthrough as it provides a fundamental solution for electrochemical detection within a microchannel in the presence of a high electric field. By virtue of the proposed design, the electrochemical detector can function regardless of where it is placed within the microchannel network including in the middle of the separation channel under a high electric field. This indicates the possibility of chemical monitoring anywhere, even under a high electric field, using a chip-based micro total analysis system consisting of multiple functional units. Further integration and miniaturization of the control peripherals and the chip itself are predicted to enable the realization of practical systems for microfluidic analysis.

ASSOCIATED CONTENT

Supporting Information

Experimental details and additional cyclic voltammograms. This material is available free of charge via the Internet at http://pubs.acs.org.

AUTHOR INFORMATION

Corresponding Author

*E-mail: tdchung@snu.ac.kr.

ACKNOWLEDGMENTS

This work was supported by the National Research Foundation of Korea (NRF) grant funded by the Korea government (MEST) (No. 2011-0001218) and by the Nano/Bio Science and Technology Program (M10536090001-05N3609-00110). Support was also provided by the Public Welfare & Safety research program (No. 2011-0021117) through the National Research Foundation (NRF) grant funded by the Ministry of Education, Science and Technology (MEST) of Korea and the Technology Development Program (109146-03-1-SB030) funded by the Ministry for Food, Agriculture, Forestry and Fisheries of Korea.

REFERENCES

(1) Kenyon, S. M.; Meighan, M. M.; Hayes, M. A. *Electrophoresis* **2011**, *32*, 482−493.
(2) Poinsot, V.; Gavard, P.; Feurer, B.; Couderc, F. *Electrophoresis* **2010**, *31*, 105−121.
(3) Tran, N. T.; Ayed, I.; Pallandre, A.; Taverna, M. *Electrophoresis* **2010**, *31*, 147−173.
(4) Lim, Y. C.; Kouzani, A. Z.; Duan, W. *Microsyst. Technol.* **2010**, *16*, 1995−2015.
(5) Arora, A.; Simone, G.; Salieb-Beugelaar, G. B.; Kim, J. T.; Manz, A. *Anal. Chem.* **2010**, *82*, 4830−4847.
(6) Chen, X. G.; Fan, L. Y.; Hu, Z. *Electrophoresis* **2004**, *25*, 3962−3969.
(7) Guihen, E.; O'Connor, W. T. *Electrophoresis* **2009**, *30*, 2062−2075.
(8) Baker, C. A.; Duong, C. T.; Grimley, A.; Roper, M. G. *Bioanalysis* **2009**, *1*, 967−975.
(9) Viskari, P. J.; Landers, J. P. *Electrophoresis* **2006**, *27*, 1797−1810.
(10) Opekar, F.; Stulik, K. *Electrophoresis* **2011**, *32*, 795−810.
(11) Gotz, S.; Karst, U. *Anal. Bioanal. Chem.* **2007**, *387*, 183−192.
(12) Kitagawa, F.; Otsuka, K. *J. Pharm. Biomed. Anal.* **2011**, *55*, 668−678.
(13) Renzi, R. F.; Stamps, J.; Horn, B. A.; Ferko, S.; VanderNoot, V. A.; West, J. A. A.; Crocker, R.; Wiedenman, B.; Yee, D.; Fruetel, J. A. *Anal. Chem.* **2005**, *77*, 435−441.
(14) Fister, J. C.; Jacobson, S. C.; Davis, L. M.; Ramsey, J. M. *Anal. Chem.* **1998**, *70*, 431−437.
(15) Wang, J. *Acc. Chem. Res.* **2002**, *35*, 811−816.
(16) Fischer, D. J.; Hulvey, M. K.; Regel, A. R.; Lunte, S. M. *Electrophoresis* **2009**, *30*, 3324−3333.
(17) Ghanim, M. H.; Abdullah, M. Z. *Talanta* **2011**, *85*, 28−34.
(18) Wallingford, R. A.; Ewing, A. G. *Anal. Chem.* **1987**, *59*, 1762−1766.
(19) Lu, W. Z.; Cassidy, R. M. *Anal. Chem.* **1994**, *66*, 200−204.
(20) Park, S.; McGrath, M. J.; Smyth, M. R.; Diamond, D.; Lunte, C. E. *Anal. Chem.* **1997**, *69*, 2994−3001.
(21) Voegel, P. D.; Zhou, W. H.; Baldwin, R. P. *Anal. Chem.* **1997**, *69*, 951−957.
(22) Xu, J. J.; Wang, A. J.; Chen, H. Y. *Trends Anal. Chem.* **2007**, *26*, 125−132.
(23) Woolley, A. T.; Lao, K. Q.; Glazer, A. N.; Mathies, R. A. *Anal. Chem.* **1998**, *70*, 684−688.
(24) Wang, J.; Tian, B. M.; Sahlin, E. *Anal. Chem.* **1999**, *71*, 5436−5440.
(25) Ertl, P.; Emrich, C. A.; Singhal, P.; Mathies, R. A. *Anal. Chem.* **2004**, *76*, 3749−3755.
(26) Rossier, J. S.; Roberts, M. A.; Ferrigno, R.; Girault, H. H. *Anal. Chem.* **1999**, *71*, 4294−4299.
(27) Amatore, C.; Da Mota, N.; Sella, C.; Thouin, L. *Anal. Chem.* **2007**, *79*, 8502−8510.
(28) Amatore, C.; Da Mota, N.; Sella, C.; Thouin, L. *Anal. Chem.* **2008**, *80*, 4976−4985.
(29) Martin, R. S.; Ratzlaff, K. L.; Huynh, B. H.; Lunte, S. M. *Anal. Chem.* **2002**, *74*, 1136−1143.

(30) Chen, C. P.; Hahn, J. H. *Anal. Chem.* **2007**, *79*, 7182−7186.
(31) Rossier, J. S.; Ferrigno, R.; Girault, H. H. *J. Electroanal. Chem.* **2000**, *492*, 15−22.
(32) Chen, D. C.; Hsu, F. L.; Zhan, D. Z.; Chen, C. H. *Anal. Chem.* **2001**, *73*, 758−762.
(33) Lacher, N. A.; Lunte, S. M.; Martin, R. S. *Anal. Chem.* **2004**, *76*, 2482−2491.
(34) Arora, A.; Eijkel, J. C. T.; Morf, W. E.; Manz, A. *Anal. Chem.* **2001**, *73*, 3282−3288.
(35) Zhan, W.; Alvarez, J.; Crooks, R. M. *J. Am. Chem. Soc.* **2002**, *124*, 13265−13270.
(36) Klett, O.; Nyholm, L. *Anal. Chem.* **2003**, *75*, 1245−1250.
(37) Ordeig, O.; Godino, N.; del Campo, J.; Munoz, F. X.; Nikolajeff, F.; Nyholm, L. *Anal. Chem.* **2008**, *80*, 3622−3632.
(38) Chun, H. G.; Chung, T. D.; Kim, H. C. *Anal. Chem.* **2005**, *77*, 2490−2495.
(39) Joo, S.; Park, S.; Chung, T. D.; Kim, H. C. *Anal. Sci.* **2007**, *23*, 277−281.
(40) Mavre, F.; Anand, R. K.; Laws, D. R.; Chow, K. F.; Chang, B. Y.; Crooks, J. A.; Crooks, R. M. *Anal. Chem.* **2010**, *82*, 8766−8774.
(41) Chang, B. Y.; Crooks, J. A.; Chow, K. F.; Mavre, F.; Crooks, R. M. *J. Am. Chem. Soc.* **2010**, *132*, 15404−15409.
(42) Dumitrescu, I.; Anand, R. K.; Fosdick, S. E.; Crooks, R. M. *J. Am. Chem. Soc.* **2011**, *133*, 4687−4689.
(43) Forry, S. P.; Murray, J. R.; Heien, M.; Locascio, L. E.; Wightman, R. M. *Anal. Chem.* **2004**, *76*, 4945−4950.
(44) Wallenborg, S. R.; Nyholm, L.; Lunte, C. E. *Anal. Chem.* **1999**, *71*, 544−549.
(45) Klett, O.; Bjorefors, F.; Nyholm, L. *Anal. Chem.* **2001**, *73*, 1909−1915.
(46) Martin, R. S.; Gawron, A. J.; Lunte, S. M.; Henry, C. S. *Anal. Chem.* **2000**, *72*, 3196−3202.
(47) Mavre, F.; Chow, K. F.; Sheridan, E.; Chang, B. Y.; Crooks, J. A.; Crooks, R. M. *Anal. Chem.* **2009**, *81*, 6218−6225.
(48) Matysik, F. M. *J. Chromatogr., A* **1996**, *742*, 229−234.
(49) Matysik, F. M. *J. Chromatogr., A* **1998**, *802*, 349−354.
(50) Cao, W. D.; Liu, J. F.; Yang, X. R.; Wang, E. *Electrophoresis* **2002**, *23*, 3683−3691.